

## PAPER

[View Article Online](#)  
[View Journal](#) | [View Issue](#)Cite this: *Dalton Trans.*, 2021, **50**, 5590Received 30th December 2020,  
Accepted 17th March 2021

DOI: 10.1039/d0dt04421k

[rsc.li/dalton](http://rsc.li/dalton)

# Oxidative degradation of toxic organic pollutants by water soluble nonheme iron(IV)-oxo complexes of polydentate nitrogen donor ligands†

Sandip Munshi, Rahul Dev Jana and Tapan Kanti Paine \*

The ability of four mononuclear nonheme iron(IV)-oxo complexes supported by polydentate nitrogen donor ligands to degrade organic pollutants has been investigated. The water soluble iron(II) complexes upon treatment with ceric ammonium nitrate (CAN) in aqueous solution are converted into the corresponding iron(IV)-oxo complexes. The hydrogen atom transfer (HAT) ability of iron(IV)-oxo species has been exploited for the oxidation of halogenated phenols and other toxic pollutants with weak X–H (X = C, O, S, etc.) bonds. The iron-oxo oxidants can oxidize chloro- and fluorophenols with moderate to high yields under stoichiometric as well as catalytic conditions. Furthermore, these oxidants perform selective oxidative degradation of several persistent organic pollutants (POPs) such as bisphenol A, nonylphenol, 2,4-D (2,4-dichlorophenoxyacetic acid) and gammexene. This work demonstrates the utility of water soluble iron(IV)-oxo complexes as potential catalysts for the oxidative degradation of a wide range of toxic pollutants, and these oxidants could be considered as an alternative to conventional oxidation methods.

## Introduction

Numerous toxic organic matters in the environment cause severe health issues to human beings and other habitants.<sup>1,2</sup> Various synthetic organic compounds having adverse effects on the environment include polychlorinated phenols (PCPs), pesticides, petroleum products, aromatic/heteroaromatic compounds, etc. (Chart 1).<sup>3</sup> Twelve such compounds have been registered as persistent organic pollutants (POPs)<sup>4,5</sup> that are toxic and resistant to biodegradation processes.<sup>6</sup> While polychlorobiphenyls (PCBs) are associated with neurotoxicity,<sup>7</sup> hydroxylated PCBs show toxicity toward wildlife and humans.<sup>8,9</sup> Pentachlorophenol, a useful substance used as a coolant in capacitors and transformers, is often released into the environment from industrial sources. Besides these PCBs, bisphenol A (BPA), nonylphenol (NP), tetrachloroethylene, DDT, and gammexene are amongst the other toxic organic pollutants which have adverse effects on humans and marine lives.<sup>10–13</sup>

Bacterial biodegradation of toxic organic compounds provides insights into the degradation of organic pollutants in soil.<sup>3</sup> While nonylphenol is biodegraded by microorganisms in water, sediment and soil,<sup>14</sup> dehydrohalogenation of lindane, a

POP, takes place in moist soil by *Clostridium sporogenes* or *Bacillus coli*.<sup>15</sup> Taking inspiration from bacterial degradation processes, advanced oxidation processes (AOPs) have been developed for efficient decomposition of organic pollutants.<sup>16–18</sup> At neutral pH, the AOPs can generate the hydroxyl radical ( $\cdot\text{OH}$ ) as the active oxidant<sup>6</sup> in the presence of transition metal ions.<sup>19–21</sup> Catalytic systems such as copper complexes under visible light irradiation,<sup>22</sup> bicarbonate-activated  $\text{H}_2\text{O}_2$  in the presence of a cobalt catalyst,<sup>23</sup> and Fe-TAML activators<sup>24,25</sup> have been developed for this purpose. Electrochemical degradation of bisphenol A by the iron(II)-activated peroxydisulfate process has been explored very recently.<sup>26</sup> Sharma *et al.* investigated the degradation of endocrine disruptors, antibiotics, anticonvulsants, and anti-inflammatory agents along with cosmetic products by ferrate ions.<sup>27</sup> Very recently, Sun *et al.* developed a method for the activation of ferrates by CNT in the degradation of bromophenol contaminants in water.<sup>28</sup> However, most of the

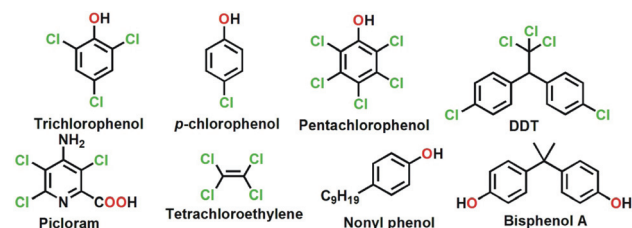
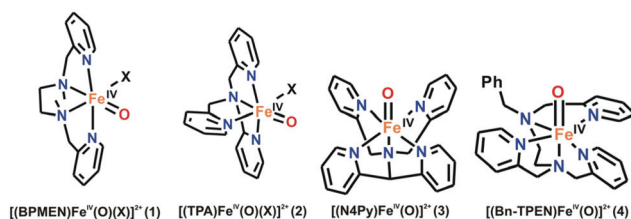


Chart 1 Common organic pollutants present in the environment.

School of Chemical Sciences, Indian Association for the Cultivation of Science,  
2A&2B Raja S. C. Mullick Road, Jadavpur, Kolkata 700032, India.

E-mail: [ictkp@iacs.res.in](mailto:ictkp@iacs.res.in)

† Electronic supplementary information (ESI) available: Crystallographic data in CIF format and spectral data of the compounds. See DOI: 10.1039/d0dt04421k



**Chart 2** Complexes used in this study. X = counterion or solvent.

methods suffer from the kinetic sluggishness of the reaction. Additionally, these catalysts work at low pH and recycling the catalysts is quite complex.<sup>29,30</sup> In this context, the development of bioinspired catalytic methods for the degradation of toxic pollutants using dioxygen or reduced oxygen species is a topic of contemporary interest.

Oxidative transformations of organic substrates in biological systems are catalyzed by dioxygen-activating mononuclear nonheme iron enzymes. Mononuclear nonheme iron(IV)-oxo species have been proposed as reactive intermediates in several biologically important oxidation reactions including biodegradation of toxic pollutants.<sup>31</sup> Inspired by the high-valent iron-oxo oxidants in biological oxidations, several synthetic nonheme iron(IV)-oxo complexes have been isolated and characterized.<sup>32–35</sup> Nonheme iron complexes allow the tuning of their reactivity by stereo-electronic modification of the supporting ligands. Over the last few years, a number of water-soluble iron complexes have been reported to form high valent iron–oxygen intermediates.<sup>36–38</sup> These complexes display versatile reactivity in terms of hydrogen atom transfer (HAT) and oxygen atom transfer (OAT) activities.<sup>39–41</sup> However, the potential of high valent metal-oxo catalysts in the oxidative degradation of pollutants has not been explored even after two decades since the synthesis of the first iron(IV)-oxo species. In this direction, we have investigated the ability of a series of water soluble nonheme iron(IV)-oxo species (Chart 2) supported by nitrogen-rich tetradentate and pentadentate ligands: TPA (tris(2-pyridylmethyl)amine), BPMEN ( $N^1, N^2$ -dimethyl- $N^1, N^2$ -bis(2-pyridylmethyl)ethane-1,2-diamine), N4Py (1,1-di(pyridin-2-yl)- $N, N$ -bis(pyridin-2-ylmethyl)methanamine) and Bn-TPEN ( $N^1$ -benzyl- $N^1, N^2, N^2$ -tris(pyridin-2-ylmethyl)ethane-1,2-diamine). These ligands have been reported to support the iron(IV)-oxo unit.<sup>42–45</sup> The high-valent iron-oxo species are generated from the respective iron(II) precursor complex in the reaction with ceric ammonium nitrate (CAN). Various toxic organic pollutants are oxidatively degraded by these metal-based oxidants. The concept of using purely metal-based oxidants in performing the oxidative degradation of toxic organic pollutants in wastewater is presented in this work.

## Results and discussion

### Generation of the iron(IV)-oxo complexes

The iron(II) complexes were oxidized to the corresponding iron(IV)-oxo species upon treatment with ceric ammonium nitrate

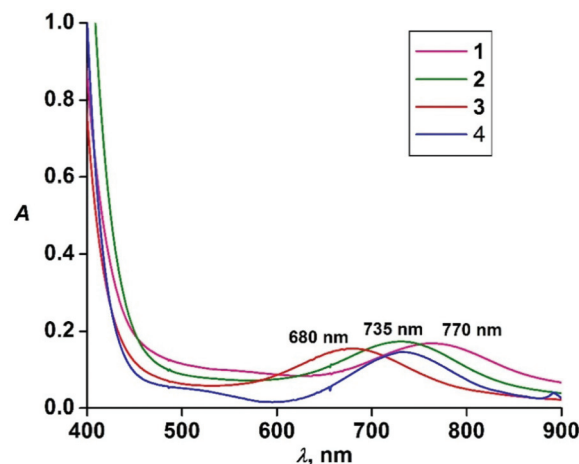


**Fig. 1** Optical spectra of the iron(IV)-oxo species (1–4) (0.5 mM in water at 298 K).

(CAN) (6 equiv.) in aqueous solution. When CAN was added to aqueous solutions of the complexes at room temperature, pale green intermediates were formed in all the cases (Fig. 1).<sup>44,46</sup> The intermediates were characterized by ESI-mass spectrometry and optical spectroscopy (see the Experimental section and Fig. S1–S4, ESI†). The absorption bands in the near-IR region bear similarities to those of the well-characterized  $S = 1$  iron(IV)-oxo complexes reported in the literature, and the position of the absorption band shifts with the number of pyridine donors on the ligand.<sup>47</sup> In addition, complex 4 was characterized by Mössbauer spectroscopy. The zero-field  $^{57}\text{Fe}$  Mössbauer spectrum of a frozen sample of complex 4 at 77 K (Fig. S5, ESI†) shows a major species with isomer shift ( $\delta$ ) and quadruple splitting ( $\Delta E_Q$ ) values of  $-0.08 \text{ mm s}^{-1}$  and  $0.71 \text{ mm s}^{-1}$ , respectively. The optical spectral data along with the Mössbauer spectral data unambiguously support the formation of iron(IV)-oxo species in aqueous solution. The iron(IV)-oxo complexes (1–4) can also be generated by using potassium peroxydisulfate (oxone) at room temperature in aqueous solution (Fig. S6, ESI†). The half-lives of the intermediates are found to be dependent not only on the geometry and electronic properties of the supporting ligands but also on the reaction conditions. The half-lives of  $[(\text{BPMEN})\text{Fe}(\text{O})]^{2+}$  (1) and  $[(\text{TPA})\text{Fe}(\text{O})]^{2+}$  (2) are 12 min and 20 min, respectively, whereas the half-lives of  $[(\text{N4Py})\text{Fe}(\text{O})]^{2+}$  (3) and  $[(\text{Bn-TPEN})\text{Fe}(\text{O})]^{2+}$  (4) are calculated to be 6 d and 1 d, respectively. The half-lives of the intermediates generated with CAN are longer than those of the intermediates generated with PhIO or oxone because of the higher stability of the iron(IV)-oxo species under acidic conditions.<sup>44</sup>

### Oxidation of sulfur containing compounds by the iron(IV)-oxo species

The oxygen atom transfer (OAT) ability of the nonheme iron(IV)-oxo complexes was tested using thioanisole as a model substrate. In each case, thioanisole oxide (Fig. S7, ESI†) was found as the sole product without the formation of the double-oxyge-

**Table 1** Time taken and yields in thioanisole oxidation by the iron(IV)-oxo oxidants

| Complex                            | 1      | 2      | 3            | 4            |
|------------------------------------|--------|--------|--------------|--------------|
| Half-life ( $t_{1/2}$ )            | 12 min | 20 min | 6 d          | 1 d          |
| Reaction time                      | 30 min | 1 h    | 16 h         | 12 h         |
| % Yield (TON) of thioanisole oxide | 76     | 60     | 120<br>(1.2) | 130<br>(1.3) |

Reaction conditions: complex : CAN : substrate = 1 : 6 : 10; 0.01 mmol of iron(II) precursor complex in water at 298 K. Yield is calculated with respect to the iron(II) complex. TON = mol of product/mol of iron complex.

nated sulfone product (Table 1).<sup>48</sup> The iron-oxo complexes of the tetradentate ligands can oxygenate thioanisole with up to 76% yield within an hour, whereas those of the pentadentate ligands display higher stoichiometric conversion after several hours. Thus, the S-containing pollutants especially heterocyclic compounds can be oxidized to less harmful sulfoxide products.

### Reaction of the iron(IV)-oxo species with chlorophenols

In the reaction between the iron(IV)-oxo species **1** and 4-chlorophenol (2 equiv.), the characteristic absorption band at 770 nm decays within 15 s with concomitant formation of a broad shoulder at around 500 nm. The absorption band at 500 nm may be attributed to phenolate to iron(III) charge transfer transitions (Fig. 2a). The faster decay of the 770 nm band compared to the self-decay rate of **1** suggests oxidative conversion of phenol during the reaction. The second order rate constant ( $k_2$ ) for the oxidation of 4-chlorophenol, obtained by varying the amount of 4-chlorophenol, is calculated to be  $363 \text{ M}^{-1} \text{ s}^{-1}$  (Fig. 2b).

With the other iron(IV)-oxo complexes (**2–4**), similar optical spectral changes are observed in the reaction with 4-chlorophenols. The  $k_2$  values with the complexes are found to be in the range of  $175\text{--}287 \text{ M}^{-1} \text{ s}^{-1}$  (Fig. S8–S10, ESI†). The rate of oxidation is faster with the iron-oxo complexes of the tetradentate ligands. Among all the complexes, the iron(IV)-oxo complex (**1**) of the BPMEN ligand shows the highest rate, whereas that of the pentadentate N4Py ligand is least reactive (Fig. 3). It should be noted that in photo-Fenton systems with iron(III), humic acid (pH = 5.0) and hydrogen peroxide, complete oxidations of PCPs take around 300 min.<sup>21</sup> In contrast, the iron-oxo complexes take only a few seconds to oxidize 4-chlorophenols. Thus, the high-valent iron-oxo systems are effective in degrading chlorophenols.

Analyses of the products after the reaction of 4-chlorophenol and **1** reveal that the substrate undergoes oxidative dechlorination (Table 2). 4-Chlorophenol is degraded to *p*-benzoquinone in a (sub)stoichiometric yield by **1** and **2**. However, higher than stoichiometric yields are observed in the oxidation by complexes **3** and **4**. The other chlorophenolic substrate, 2,4,6-trichlorophenol, is selectively converted into 2,6-dichloro-*p*-benzoquinone by complexes **1** and **2** with 1.5 and 1.0 turnover numbers (TONs), respectively (Fig. S11 and S12,

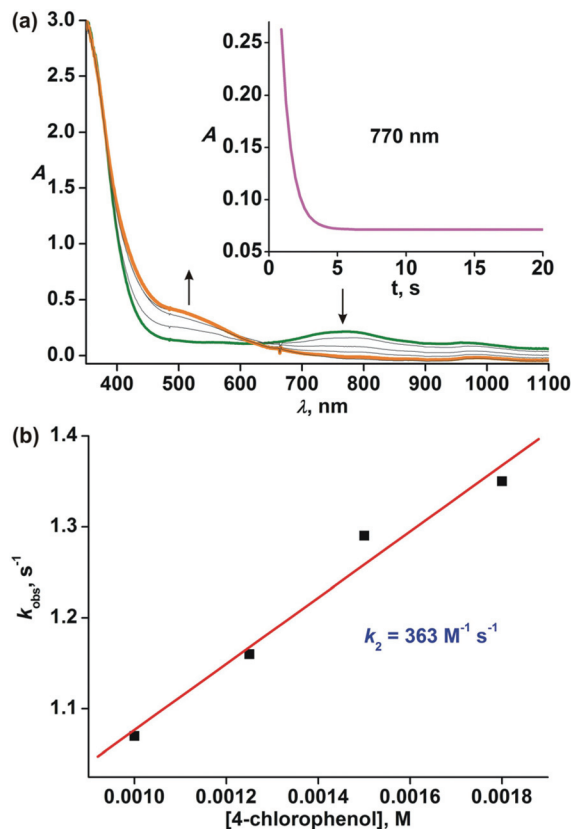


**Fig. 2** (a) Optical spectral changes with time during the reaction between **1** (0.5 mM in acetonitrile) and 4-chlorophenol (1 mM) at 298 K. Inset: Time trace for the 770 nm band. (b) Second order rate constant for 4-chlorophenol oxidation by **1**.

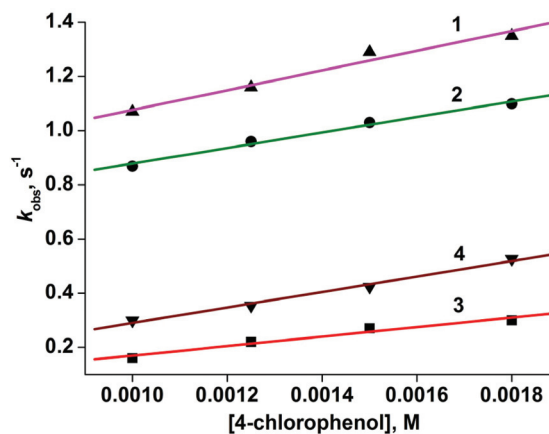


**Fig. 3** Second order rate constants for 4-chlorophenol oxidation by the iron(IV)-oxo complexes at 298 K.

ESI†). The iron-oxo complexes **3** and **4** oxidize 2,4,6-trichlorophenol to 2,6-dichloro-*p*-benzoquinone as the major product along with the minor product 2,6-dihydroxy-*p*-benzoquinone (Table 2). The chlorine atoms of chlorophenols remain as chloride ions ( $\text{Cl}^-$ ) after the reaction, which has been confirmed by the silver nitrate test. The presence of chloride ions

**Table 2** Yields of products derived from chloro- and fluorophenols in the oxidative dechlorination by the iron(IV)-oxo oxidants

| Substrate             | Product                                     | % Yield (TON) |     |           |           |
|-----------------------|---------------------------------------------|---------------|-----|-----------|-----------|
|                       |                                             | 1             | 2   | 3         | 4         |
| 4-Chlorophenol        | <i>p</i> -Benzoquinone                      | 94            | 84  | 170 (1.7) | 180 (1.8) |
| 2,4,6-Trichlorophenol | 2,6-Dichloro- <i>p</i> -benzoquinone        | 150 (1.5)     | 100 | 90        | 130 (1.3) |
|                       | 2,6-Dihydroxy- <i>p</i> -benzoquinone       | —             | —   | 32        | 50        |
| Pentafluorophenol     | 2,3,5,6-Tetrafluoro- <i>p</i> -benzoquinone | 70            | 55  | 20        | 75        |

Reaction conditions: complex:CAN:substrate = 1:6:10; 0.01 mmol of iron(II) precursor complex in water at 298 K. Yield is calculated with respect to the iron(II) complex. TON = mol of product/mol of iron complex.

in the final solution clearly points toward the two-electron oxidation of chlorophenols and rules out the possibility of any radical reactions.

With the increasing amount of CAN, the catalytic efficiency of the complexes in the degradation of chlorophenols increases. When the reaction is carried out with 60 equiv. of CAN, 2,4,6-trichlorophenol is degraded catalytically with a maximum TON of 12, whereas 4-chlorophenol is converted into *p*-benzoquinone with a TON of 25 by complex 3 (Fig. 4). This outcome clearly signifies the role of high valent iron-oxo species in affecting oxidative dehalogenation reactions.

Thus the nonheme iron(IV)-oxo complexes can degrade PCPs catalytically in aqueous medium. Most of the earlier reports on the degradation of PCPs rely on Fenton-type chemistry, by which PCPs are converted into more toxic biphenyl compounds *via* the one-electron oxidation process.<sup>21,28</sup> In contrast, the iron(II)/CAN/H<sub>2</sub>O systems presented here selectively oxidize PCPs to less toxic quinones *via* the two-electron oxidation process and the iron(IV)-oxo oxidants revert to the corresponding iron(II) precursor displaying catalytic activity.

### Reaction of the iron-oxo species with fluorophenols

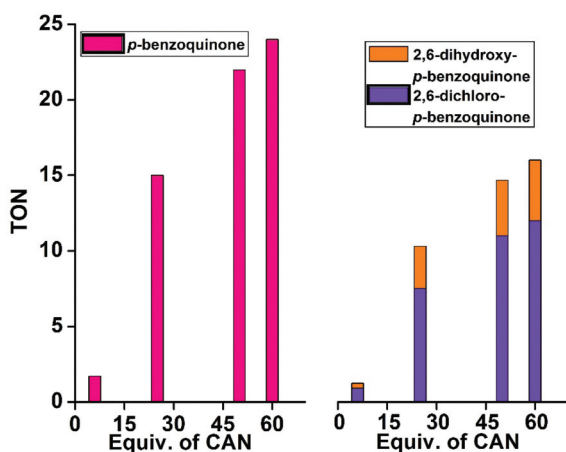
Fluorinated compounds are one of the major harmful contaminants in aqueous medium. They are exceptionally difficult to degrade. In nature, several enzymes carry out the breakdown

of C–F bonds, *e.g.*, fluoroacetate dehalogenase, fluoroacetate-specific defluorinase, and 4-fluorobenzoate dehalogenase.<sup>49,50</sup> The radical Fenton processes are not efficient in breaking strong C–F bonds. Sorokin *et al.* reported the oxidative defluorination of fluorinated aromatic compounds by high valent iron-porphyrin compounds.<sup>51,52</sup> The iron-oxo species reported in this work not only perform the oxidative degradation of chlorophenols, but are equally effective in the oxidative defluorination of fluorophenols (Table 2). The high valent iron-based oxidants carry out the degradation of fluorinated phenols to benzoquinone. Pentafluorophenol is selectively oxidized to 2,3,5,6-tetrafluoro-*p*-benzoquinone by complexes 1, 2, 3 and 4 with 70%, 55%, 20% and 75% yields, respectively (Fig. S13 and S14, ESI†).

Furthermore, the catalytic activity of the complexes has been investigated towards the defluorination reactions in the presence of 60 equiv. of CAN. However, the catalytic efficiency of the complexes in the defluorination reaction is lower compared to the dechlorination reaction. The maximum TONs of 2 and 5.2 were observed for 2,3,5,6-tetrafluoro-*p*-benzoquinone by 2 and 4, respectively (Fig. S15, ESI†).

### Reaction of the iron(IV)-oxo species with POPs

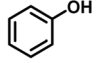
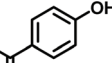
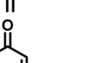
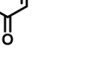
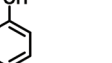
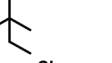
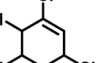
Using the strategy for the oxidation of PCPs, the oxidizing ability of the iron(IV)-oxo complexes was tested in the degradation of more toxic and environmentally hazardous substances. The iron(IV)-oxo species are capable of degrading bisphenol A to phenols in good yields. The yields vary in the range of 40–75% depending on the oxidizing capacity of the complexes (Table 3). The end product of the reaction is phenol or substituted phenol (Fig. S16–S18, ESI†); these products are much less toxic and biodegradable and can be degraded further by the oxidants. Nonylphenol is also degraded by these high valent iron-oxo oxidants to substituted phenol and benzoquinone in 30–40% yields (Fig. S19 and S20, ESI†) (Table 3). In addition, the iron-based oxidants can dehalogenate lindane (commercially known as gammaxene), an insecticide, to form pentachlorocyclohexene (Fig. 5 and Fig. S21, ESI†) but with low yields (Table 3). The reason for the low yields is the high C–H bond energy of this cyclohexane derivative, as the iron(IV)-oxo species performs the hydrogen atom abstraction reaction from C–H bonds for this kind of substrate.



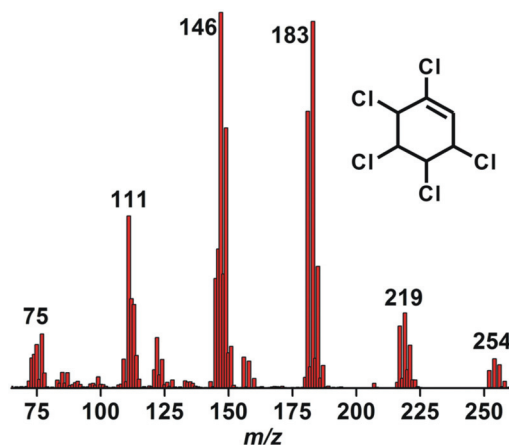
**Fig. 4** Catalytic oxidation of 4-chlorophenol (left) and 2,4,6-trichlorophenol (right) by 3 (0.01 mmol) using CAN (60 equiv.) at 298 K.



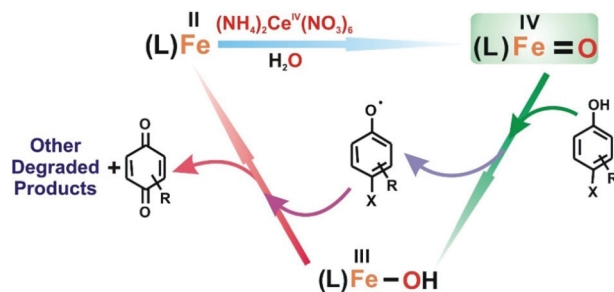
**Table 3** Products derived from different pollutants by the iron(IV)-oxo complexes

| Substrate                       | Product                                                                           | % Yield |    |    |    |
|---------------------------------|-----------------------------------------------------------------------------------|---------|----|----|----|
|                                 |                                                                                   | 1       | 2  | 3  | 4  |
| Bisphenol A                     |  | 18      | 11 | 21 | 32 |
|                                 |  | 39      | 35 | 50 | 75 |
| Nonylphenol                     |  | 40      | 36 | 18 | 45 |
|                                 |  | 30      | 13 | 19 | 35 |
| Lindane                         |  | 8       | 6  | 4  | 6  |
| 2,4-dichlorophenoxy acetic acid |  | 40      | 91 | 38 | 57 |
|                                 |  |         |    |    |    |

Reaction conditions: complex : CAN : substrate = 1 : 6 : 10; 0.01 mmol of iron(II) precursor complex in the acetonitrile:water (9 : 1) mixture at 298 K. Yield is calculated with respect to the iron(II) complex.

**Fig. 5** GC-mass spectrum of pentachlorocyclohexene formed in the reaction of **1** with lindane (10 equiv.).

2,4-Dichlorophenoxyacetic acid (2,4-D), a widely used herbicide, can be oxidized by the high valent iron(IV)-oxo species.<sup>53</sup> Complex **2** oxidatively converts 2,4-dichlorophenoxyacetic acid

**Scheme 1** Proposed pathway of the oxidative degradation of pollutants by iron(IV)-oxo complexes. "L" stands for the tetradentate or pentadentate supporting ligand.

into the corresponding dichlorophenol with 91% yield. The yields are found to be 57%, 38% and 40% in the case of **4**, **3** and **1**, respectively (Table 3). It is important to note that the product 2,4-dichlorophenol (Fig. S22 and S23, ESI†) is also a substrate for the iron-oxo oxidants. The oxidizing ability of the iron(IV)-oxo complexes, generated by oxone, has also been investigated with 2,4-D as the substrate. 2,4-D is oxidized to 2,4-dichlorophenol with 44% and 75% yields by complexes **1** and **3**, respectively. Therefore, it can be concluded that the reported iron(IV)-oxo complexes can perform oxidative degradation of the toxic substances irrespective of the oxidant used for the generation of these iron(IV)-oxo species.

The nonheme iron(IV)-oxo complexes degrade different types of organic pollutants by HAT reactions, a common pathway invoked for iron(IV)-oxo species.<sup>54</sup> These oxidants can perform epoxidation of alkenes, oxyfunctionalization of the C–H bonds and abstraction of the H atom from phenol groups. Therefore, the pollutants bearing such functional groups can easily be degraded. The metal-based active oxidants can abstract the H atom from the O–H bond of the phenolic substrates. The resulting iron(III)-OH species then combines with the phenoxyl radical and reverts to iron(II) in the catalytic cycle (Scheme 1).

## Experimental

### Methods and equipment

All reagents were purchased from commercial sources and were used without further purification, unless otherwise mentioned. Solvents were distilled, dried and deoxygenated before use. The preparation and handling of air-sensitive iron(II) compounds were carried out under an inert atmosphere in a glove box. Although no problem was encountered during the synthesis of the complexes, perchlorate salts are potentially explosive and should be handled with care. The ligands were synthesized according to the procedures reported in the literature.<sup>55–57</sup> The precursor iron(II) complexes, [(BPMEN)Fe<sup>II</sup>(OTf)<sub>2</sub>], [(TPA)Fe<sup>II</sup>(OTf)<sub>2</sub>], [(N4Py)Fe<sup>II</sup>(CH<sub>3</sub>CN)](ClO<sub>4</sub>)<sub>2</sub> and [(Bn-TPEN)Fe<sup>II</sup>(OTf)<sub>2</sub>], were prepared according to the reported procedures.<sup>44,46</sup>

Single and time-dependent electronic spectra in solutions were obtained on an Agilent 8453 diode array spectrophotometer. Electrospray mass spectra were recorded on a Waters QTOF Micro YA263 spectrometer. The spectra were normalized against the most intense peak having an intensity of 100%. The Mössbauer spectrum was recorded with a  $^{57}\text{Co}$  source in a Rh matrix using an alternating constant acceleration Wissel Mössbauer spectrometer operated in the transmission mode using a Janis Research SuperVariTemp cryostat. Isomer shifts are given relative to iron metal foil at ambient temperature. Simulation of the experimental data was performed using the Igor Pro 8 program. All NMR spectra were recorded on a Bruker DPX-500/300 MHz spectrometer. GC-MS measurements were carried out with a PerkinElmer Clarus 600 chromatograph using an Elite 5 MS column (30 m  $\times$  0.25 mm  $\times$  0.25  $\mu\text{m}$ ) at a maximum temperature of 300  $^{\circ}\text{C}$ .

### Characterization of the iron(IV)-oxo complexes (1–4)

To an aqueous solution (0.5 mM) of the iron(II) complex, ceric ammonium nitrate (CAN) (6 equiv. dissolved in water) was added at 298 K. A pale green species corresponding to the iron(IV)-oxo complex was formed immediately. The reactive species were not isolated as solids, but were characterized in solution.

**[(BPMEN)Fe<sup>IV</sup>(O)]<sup>2+</sup> (1).** ESI-MS (+ve ion mode in H<sub>2</sub>O):  $m/z$  = 491.06 for  $\{[\text{Fe}(\text{O})(\text{BPMEN})](\text{OTf})\}^+$ . UV-vis:  $\lambda_{\text{max}}$  (in H<sub>2</sub>O at 298 K) = 770 nm ( $\epsilon \sim 370 \text{ M}^{-1} \text{ cm}^{-1}$ ).

**[(TPA)Fe<sup>IV</sup>(O)]<sup>2+</sup> (2).** ESI-MS (+ve ion mode in H<sub>2</sub>O):  $m/z$  = 511.08 for  $\{[\text{Fe}(\text{O})(\text{TPA})](\text{OTf})\}^+$ . UV-vis:  $\lambda_{\text{max}}$  (in H<sub>2</sub>O at 298 K) = 735 nm ( $\epsilon \sim 350 \text{ M}^{-1} \text{ cm}^{-1}$ ).

**[(N4Py)Fe<sup>IV</sup>(O)]<sup>2+</sup> (3).** ESI-MS (+ve ion mode in H<sub>2</sub>O):  $m/z$  = 219.54 for  $\{[\text{Fe}(\text{O})(\text{N4Py})]\}^+$ . UV-vis:  $\lambda_{\text{max}}$  (in H<sub>2</sub>O at 298 K) = 690 nm ( $\epsilon \sim 450 \text{ M}^{-1} \text{ cm}^{-1}$ ).

**[(Bn-TPEN)Fe<sup>IV</sup>(O)]<sup>2+</sup> (4).** ESI-MS (+ve ion mode in H<sub>2</sub>O):  $m/z$  = 644.13 for  $\{[\text{Fe}(\text{O})(\text{Bn-TPEN})](\text{OTf})\}^+$ . UV-vis:  $\lambda_{\text{max}}$  (in H<sub>2</sub>O at 298 K) = 735 nm ( $\epsilon \sim 340 \text{ M}^{-1} \text{ cm}^{-1}$ ). Zero-field  $^{57}\text{Fe}$  Mössbauer spectrum:  $\delta = -0.08 \text{ mm s}^{-1}$  and  $\Delta E_{\text{q}} = 0.71 \text{ mm s}^{-1}$ .

### Kinetic study of phenol oxidation by the iron(IV)-oxo complexes

Iron(IV)-oxo complexes were generated *in situ* by adding CAN (6 equiv.) to an acetonitrile solution of the precursor iron(II) complex (0.5 mM–1.0 mM). After de-aeration of the solutions and temperature equilibration at 25  $^{\circ}\text{C}$  in a UV-vis cuvette, the substrate was added to the solution under stirring. The concentration of the substrate was maintained in the range of 10 mM–400 mM. The time course of the decay was then monitored at 298 K by UV-vis spectroscopy. Time courses were subjected to pseudo-first-order fit, and second order rate constants were evaluated from the concentration dependence data.

### Reactions of the iron(IV)-oxo complexes with phenols

The iron(II) complex (0.01 mmol) was dissolved in water (0.8 mL). To the solution was added the substrate (10 equiv. dissolved in 0.1 mL water) followed by the addition of 0.1 mL aqueous solution of CAN (6 equiv.). The reaction solution was stirred at 298 K. At the end of the reaction, the organic pro-

ducts were extracted with diethyl ether, dried over anhydrous sodium sulfate, filtered and evaporated to dryness. The products were analyzed by  $^1\text{H}$  NMR spectroscopy using 1,3,5-trimethoxybenzene as an internal standard and/or GC-MS using naphthalene as a standard.

### Catalytic reactions of the iron(IV)-oxo complexes with phenols

The iron(II) complex (0.01 mmol) was dissolved in water (1.6 mL). To the solution was added the substrate (100 equiv. dissolved in 0.2 mL acetonitrile) followed by the addition of 0.2 mL aqueous solution of CAN (60 equiv.). The reaction solution was stirred at 298 K. At the end of the reaction, the organic products were extracted with diethyl ether, dried over anhydrous sodium sulfate, filtered and evaporated to dryness. The products were analyzed by  $^1\text{H}$  NMR spectroscopy using 1,3,5-trimethoxybenzene as an internal standard and/or GC-MS using naphthalene as a standard.

### Reactions of the iron(IV)-oxo complexes with POPs

The iron(II) complex (0.01 mmol) was dissolved in water (0.8 mL). To the solution was added the substrate (10 equiv. dissolved in 0.1 mL acetonitrile) followed by the addition of 0.1 mL aqueous solution of CAN (6 equiv.). The reaction solution was stirred at 298 K. At the end of the reaction, the organic products were extracted with diethyl ether. The products were analyzed by GC-MS using naphthalene as a standard.

### Control experiments

Control experiments were carried out with iron(II) triflate and CAN following the procedure described above. Trace amounts of oxidized products from some substrates were formed. This yield was subtracted while calculating the yield of products in the oxidation by the iron complex. Control experiments were also conducted under catalytic conditions.

## Conclusions

With an objective to develop bioinspired metal-based oxidants for the oxidative degradation of organic pollutants, four iron(II) complexes supported by nitrogen-rich tetradentate and pentadentate ligands were investigated. The iron(II) complexes generate the corresponding iron(IV)-oxo species in aqueous solution using ceric ammonium nitrate (CAN) as the oxidant. The high valent iron-oxo species, thus generated, act as potential catalysts for the oxidative degradation of divergent organic pollutants in moderate to good yields. This study provides useful insights into the development of effective green catalysts and metal-based catalytic systems to replace the traditional oxidants based on Fenton-type chemistry in the oxidative degradation of toxic organic pollutants. Further studies on the development of more reactive, oxidatively robust and recyclable metal-based oxidants for the degradation of toxic organic compounds are being carried out in our laboratory.

## Conflicts of interest

There are no conflicts to declare.

## Acknowledgements

TKP gratefully acknowledges the Science and Engineering Research Board (SERB), India (project: CRG/2019/006393) for financial support and the Technical Research Center (TRC) at IACS for infrastructural and financial support. SM and RDJ thank the Council of Scientific and Industrial Research (CSIR), India for research fellowships.

## Notes and references

- 1 C. Sun, C. Chen, W. Ma and J. Zhao, *Phys. Chem. Chem. Phys.*, 2011, **13**, 1957–1969.
- 2 R. P. Schwarzenbach, B. I. Escher, K. Fenner, T. B. Hofstetter, C. A. Johnson, U. von Gunten and B. Wehrli, *Science*, 2006, **313**, 1072–1077.
- 3 M. McGuinness and D. Dowling, *Int. J. Environ. Res. Public Health*, 2009, **6**, 2226–2247.
- 4 P. L. Lallas, *Am. J. Int. Law*, 2001, **95**, 692–708.
- 5 I. Ali, M. Asim and T. A. Khan, *J. Environ. Manage.*, 2012, **113**, 170–183.
- 6 A. Kubacka, M. Fernandez-Garcia and G. Colon, *Chem. Rev.*, 2012, **112**, 1555–1614.
- 7 E. Uwimana, X. Li and H.-J. Lehmler, *Environ. Sci. Technol.*, 2018, **52**, 6000–6008.
- 8 R. Tehrani and B. Van Aken, *Environ. Sci. Pollut. Res.*, 2014, **21**, 6334–6345.
- 9 F. A. Grimm, D. Hu, I. Kania-Korwel, H.-J. Lehmler, G. Ludewig, K. C. Hornbuckle, M. W. Duffel, Å. Bergman and L. W. Robertson, *Crit. Rev. Toxicol.*, 2015, **45**, 245–272.
- 10 S. Preethi, K. Sandhya, D. E. Lebonah, C. V. Prasad, B. Sreedevi, K. Chandrasekhar and J. P. Kumari, *Int. Lett. Nat. Sci.*, 2014, **27**, 32–46.
- 11 W. Zhang, K. Yin and L. Chen, *Appl. Microbiol. Biotechnol.*, 2013, **97**, 5681–5689.
- 12 R. Goldman, L. Enewold, E. Pellizzari, J. B. Beach, E. D. Bowman, S. S. Krishnan and P. G. Shields, *Cancer Res.*, 2001, **61**, 6367–6371.
- 13 A. Soares, B. Guieysse, B. Jefferson, E. Cartmell and J. N. Lester, *Environ. Int.*, 2008, **34**, 1033–1049.
- 14 Z. Mao, X.-F. Zheng, Y.-Q. Zhang, X.-X. Tao, Y. Li and W. Wang, *Int. J. Mol. Sci.*, 2012, **13**, 491–505.
- 15 M. N. Rashed, *Organic Pollutants-Monitoring, Risk and Treatment*, 2013, pp. 167–194.
- 16 M. Zhang, C. Chen, W. Ma and J. Zhao, *Angew. Chem., Int. Ed.*, 2008, **47**, 9730–9733.
- 17 P. R. Gogate and A. B. Pandit, *Adv. Environ. Res.*, 2004, **8**, 501–551.
- 18 B. Meunier and A. Sorokin, *Acc. Chem. Res.*, 1997, **30**, 470–476.
- 19 A. Sorokin, S. De Suzzoni-Dezard, D. Poullain, J.-P. Noël and B. Meunier, *J. Am. Chem. Soc.*, 1996, **118**, 7410–7411.
- 20 G. Upelaar, R. T. Meijers, R. Hopman and J. C. Kruithof, *Ozone: Sci. Eng.*, 2000, **22**, 607–616.
- 21 M. Fukushima and K. Tatsumi, *Environ. Sci. Technol.*, 2001, **35**, 1771–1778.
- 22 Q. Song, M. Jia, W. Ma, Y. Fang and Y. Huang, *Sci. China: Chem.*, 2013, **56**, 1775–1782.
- 23 L. Zhou, W. Song, Z. Chen and G. Yin, *Environ. Sci. Technol.*, 2013, **47**, 3833–3839.
- 24 N. Chahbane, D.-L. Popescu, D. A. Mitchell, A. Chanda, D. Lenoir, A. D. Ryabov, K.-W. Schramm and T. J. Collins, *Green Chem.*, 2007, **9**, 49–57.
- 25 S. Kundu, A. Chanda, S. K. Khetan, A. D. Ryabov and T. J. Collins, *Environ. Sci. Technol.*, 2013, **47**, 5319–5326.
- 26 C.-w. Yang, *Water Sci. Eng.*, 2015, **8**, 139–144.
- 27 V. K. Sharma, L. Chen and R. Zboril, *ACS Sustainable Chem. Eng.*, 2016, **4**, 18–34.
- 28 S. Sun, J. Jiang, L. Qiu, S. Pang, J. Li, C. Liu, L. Wang, M. Xue and J. Ma, *Water Res.*, 2019, **156**, 1–8.
- 29 S. Navalon, M. Alvaro and H. Garcia, *Appl. Catal., B*, 2010, **99**, 1–26.
- 30 R. Gonzalez-Olmos, M. J. Martin, A. Georgi, F.-D. Kopinke, I. Oller and S. Malato, *Appl. Catal., B*, 2012, **125**, 51–58.
- 31 S. C. Peck and W. A. van der Donk, *J. Biol. Inorg. Chem.*, 2017, **22**, 381–394.
- 32 W. Nam, Y. M. Lee and S. Fukuzumi, *Acc. Chem. Res.*, 2014, **47**, 1146–1154.
- 33 K. Warm, A. Paskin, U. Kuhlmann, E. Bill, M. Swart, M. Haumann, H. Dau, P. Hildebrandt and K. Ray, *Angew. Chem., Int. Ed.*, 2020, **60**, 6752–6756.
- 34 V. A. Larson, B. Battistella, K. Ray, N. Lehnert and W. Nam, *Nat. Rev. Chem.*, 2020, **4**, 404–419.
- 35 A. R. McDonald and L. Que, Jr., *Coord. Chem. Rev.*, 2013, **257**, 414–428.
- 36 T. Chantarojsiri, Y. Sun, J. R. Long and C. J. Chang, *Inorg. Chem.*, 2015, **54**, 5879–5887.
- 37 S. J. Yang and W. Nam, *Inorg. Chem.*, 1998, **37**, 606–607.
- 38 T. Funabiki, D. Sugio, N. Inui, M. Maeda and Y. Hitomi, *Chem. Commun.*, 2002, 412–413.
- 39 S. T. Kleespies, W. N. Oloo, A. Mukherjee and L. Que, Jr., *Inorg. Chem.*, 2015, **54**, 5053–5064.
- 40 C. V. Sastri, J. Lee, K. Oh, Y. J. Lee, J. Lee, T. A. Jackson, K. Ray, H. Hirao, W. Shin, J. A. Halfen, J. Kim, L. Que, Jr., S. Shaik and W. Nam, *Proc. Natl. Acad. Sci. U. S. A.*, 2007, **104**, 19181–19186.
- 41 M. S. Seo, N. H. Kim, K.-B. Cho, J. E. So, S. K. Park, M. Clémancey, R. Garcia-Serres, J.-M. Latour, S. Shaik and W. Nam, *Chem. Sci.*, 2011, **2**, 1039–1045.
- 42 J. Kaizer, E. J. Klinker, N. Y. Oh, J.-U. Rohde, W. J. Song, A. Stubna, J. Kim, E. Münck, W. Nam and L. Que, Jr., *J. Am. Chem. Soc.*, 2004, **126**, 472–473.
- 43 O. V. Makhlynets and E. V. Rybak-Akimova, *Chem. – Eur. J.*, 2010, **16**, 13995–14006.

- 44 Y. M. Lee, S. N. Dhuri, S. C. Sawant, J. Cho, M. Kubo, T. Ogura, S. Fukuzumi and W. Nam, *Angew. Chem., Int. Ed.*, 2009, **48**, 1803–1806.
- 45 M. Martinho, F. Banse, J.-F. Bartoli, T. A. Mattioli, P. Battioni, O. Horner, S. Bourcier and J.-J. Girerd, *Inorg. Chem.*, 2005, **44**, 9592–9596.
- 46 J. L. Fillol, Z. Codolà, I. Garcia-Bosch, L. Gómez, J. J. Pla and M. Costas, *Nat. Chem.*, 2011, **3**, 807–813.
- 47 M. Mitra, H. Nimir, S. Demeshko, S. S. Bhat, S. O. Malinkin, M. Haukka, J. Lloret-Fillol, G. C. Lisensky, F. Meyer, A. A. Shteinman, W. R. Browne, D. A. Hrovat, M. G. Richmond, M. Costas and E. Nordlander, *Inorg. Chem.*, 2015, **54**, 7152–7164.
- 48 R. Singh, G. Ganguly, S. O. Malinkin, S. Demeshko, F. Meyer, E. Nordlander and T. K. Paine, *Inorg. Chem.*, 2019, **58**, 1862–1876.
- 49 Y. Wang and A. Liu, *Chem. Soc. Rev.*, 2020, **49**, 4906–4925.
- 50 H. J. Seong, S. W. Kwon, D.-C. Seo, J.-H. Kim and Y.-S. Jang, *Appl. Biol. Chem.*, 2019, **62**, 62.
- 51 C. Colombar, A. H. Tobing, G. Mukherjee, C. V. Sastri, A. B. Sorokin and S. P. de Visser, *Chem. – Eur. J.*, 2019, **25**, 14320–14331.
- 52 C. Colombar, E. V. Kudrik, P. Afanasiev and A. B. Sorokin, *J. Am. Chem. Soc.*, 2014, **136**, 11321–11330.
- 53 D. Sheet and T. K. Paine, *Chem. Sci.*, 2016, **7**, 5322–5331.
- 54 W. Nam, *Acc. Chem. Res.*, 2007, **40**, 522–531.
- 55 G. J. P. Britovsek, J. England and A. J. P. White, *Inorg. Chem.*, 2005, **44**, 8125–8134.
- 56 L. Duellund, R. Hazell, C. J. McKenzie, L. P. Nielsen and H. Toftlund, *J. Chem. Soc., Dalton Trans.*, 2001, 152–156.
- 57 M. Lubben, A. Meetsma, E. C. Wilkinson, B. Feringa and L. Que, Jr., *Angew. Chem., Int. Ed.*, 1995, **34**, 1512–1514.